WATER PERMEATION THROUGH GRAPHENE NANOSLIT BY MOLECULAR DYNAMICS SIMULATION

Taro Yamada[1] and Ryosuke Matsuzaki[2]

[1] Department of Mechanical Engineering, Tokyo University of Science,
2641 Yamazaki, Noda, Chiba 278-8510, Japan
Email: 7513131@ed.tus.ac.jp

[2] Department of Mechanical Engineering, Tokyo University of Science,
2641 Yamazaki, Noda, Chiba 278-8510, Japan
Email: rmatsuza@rs.tus.ac.jp, web page: http://www.rs.tus.ac.jp/rmatsuza/index_en.html

Keywords: Graphene, Permeation, Molecular dynamics, Water transport, Knudsen

ABSTRACT

In this study, to elucidate flow mechanisms at the nanoscale, we conducted water-permeation simulation for graphene slits. In nanoscale flows, the influence of the channel wall is relatively large, and it has been confirmed that the traditional continuum model based on continuity equations fail to provide accurate predictions. Usually, the Knudsen number (*Kn*) is used to show the applicability of the continuum laws. However, the applicability of this dimensionless parameter is experimentally established, and the exact value at which deviation occurs and the reason for the deviation cannot be explained. We calculated the permeability of the flow through a slit by using classical molecular dynamics (MD) for various *Kn*, and compared the MD simulation results with predictions obtained from the continuum model. We considered two hydrodynamic models: one for a non-slip condition with velocity = 0 on the wall, and another for a slip condition with finite velocity u_s on the wall, where the velocity is proportional to pressure difference before and after permeation. The permeability values determined from MD results agree well with the results of the slip model in the range $Kn < 0.375$, but the values differed in the range $Kn > 0.375$. Additionally, from the density profile, we found that water molecules passing through a slit form high-density layers at a certain distance from the wall. When the numbers decreases to one, the flow changes from a slip flow to a free-molecular flow. This study provides guidelines for understanding flow mechanisms at the nanoscale and for the development of graphene filtration membranes.

1 INTRODUCTION

Graphene is an allotrope of carbon and has a stable, one-atom-thick, two-dimensional (2D) structure. Because the 2D structure allows electrons to move only in the plane of the material, graphene has excellent characteristics, including mechanical strength, chemical stability, thermal conductivity, and electrical conductivity. The recent improvements in manufacturing techniques (e.g., chemical vapor deposition and ultrasonication) have enabled the inexpensive fabrication of single-layer graphene. Graphene is also used in a wide range of composite materials, such as electrode materials[1], biomaterials[2], and construction materials[3].

The use of graphene in the form of nanoscale membranes such as those in mechanical pressure sensors and cell compartments has been explored because graphene has extremely low surface friction. It exhibits high permeability in the case of water, and therefore, its use in atomic-filtration, e.g., desalination and ion separation, is also investigated. For example, Geim et al.[4] fabricated graphene membranes and evaluated their permeability to water and other liquids. They found that the graphene membranes were almost impermeable to gases such as helium, but did not impede the permeation of liquid water, which permeated through the membrane 10^{10} times faster than other liquids. Additionally, because graphene has the advantage that it can be functionalized by chemical functionalization, it can be used as a laminated composite material membrane in combination with polymers. In such a composite material membrane, the polymers act as fillers, and various properties can be imparted to the composite

depending on combination of polymers. Therefore, graphene composite material membranes have gained considerable attention.

However, at the nanoscale, the influence of the channel walls is relatively large. Experimental studies confirmed that the traditional continuum equations and non-slip boundary conditions fail to provide accurate predictions[5]. For graphene composite membranes, these models are probably inappropriate for predicting permeability, and the actual performance of such membranes may differ from the expected performance. Usually, the Knudsen number (*Kn*) is used to determine the applicability of the continuum laws to nanoscale flows. Nevertheless, *Kn* only shows the flow form obtained from experiments and does not accurately show the applicable limit value of continuum laws.

Thus, we conducted MD simulations of the water flow through graphene-slit structures to investigate the applicable limitation value of the continuum laws. We calculated permeability values using the results of the MD simulations and compared these values with predictions based on non-slip and slip models.

2 HYDRODYNAMIC MODEL

2.1 Knudsen number

We consider the flow through single-layer graphene slits, as shown in Figure. 1. For a nanoscale flow, the non-dimensional *Kn* indicates the applicability of fluid mechanics. It is defined as follows:

$$Kn = \frac{\lambda}{L_s}, \tag{1}$$

where λ is the mean free path of fluid molecules, and L_s is the characteristic channel dimension. We substitute λ with the lattice spacing for water δ (= 0.3 nm) because defining λ for liquid water is difficult. We use the slit width d as L_s. The relationships between *Kn* and flow form are known; they are presented in Table 1[6]. We focus on the range of d from 0.464 to 3.16 nm (i.e., $0.095 < Kn < 0.6$), which is the transition regime. In this regime, as d increases, the flow is expected to exhibit a slip tendency, and as d decreases, the flow is expected to exhibit a free-molecular flow tendency, and the applicability of the slip flow decreases.

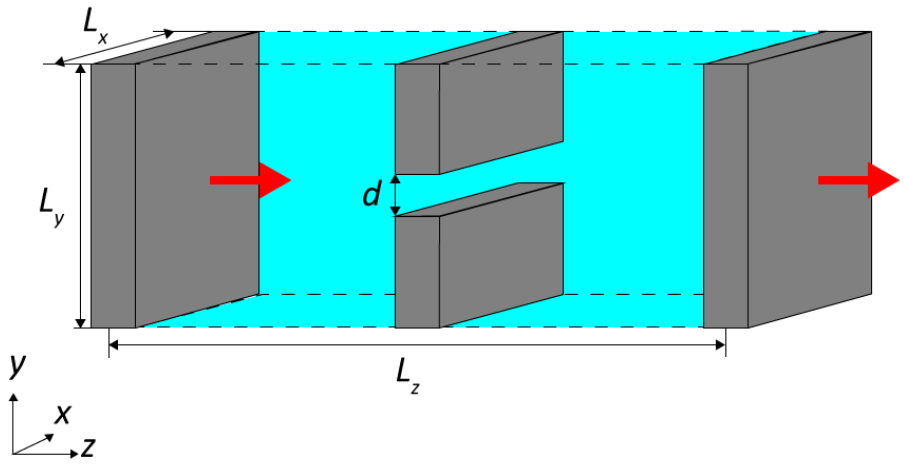

Figure. 1: Schematic of the computational setup.

Kn	Flow condition	Continuum mechanics
$Kn < 10^{-3}$	Continuum flow	Applicable
$10^{-3} < Kn < 10^{-1}$	Slip flow	Applicable
$10^{-1} < Kn < 10$	Transition regime	Not applicable
$10 < Kn$	Free-molecular flow	Not applicable

Table1: Knudsen number regimes.

2.2 Permeability

Permeability is equal to the ratio of the flux through a membrane Q to the transmembrane pressure difference ΔP. It is used as an indicator of the ease with which fluid can pass through a membrane. To calculate permeability using MD, we consider it as the linearly approximated pressure-gradients obtained from the MD simulations with various ΔP.

$$K_{MD} = \frac{Q}{\Delta P}. \tag{2}$$

We consider two hydrodynamic models: the non-slip condition and slip condition with finite velocity u_s on the wall, where the velocity is proportional to the pressure difference before and after permeation. By solving the continuum-dynamics equations for 2D slits of width d and with velocity = 0 at the wall, the theoretical permeance for the non-slip model is written as follows[7]:

$$K_{non-slip} = \frac{\pi d^2}{32\mu}, \tag{3}$$

where μ is the viscosity of the fluid, and $K_{\text{non-slip}}$ is the theoretical permeance for the non-slip model. For the slip condition, slip velocity u_s at the solid-liquid interface is proportional to ΔP with the proportionality constant α.

$$u_s = \alpha \Delta P. \tag{4}$$

Using this velocity u_s as the boundary condition on the wall, the theoretical permeance for the slip model can be written as follows:

$$K_{slip} = \frac{\pi d^2}{32\mu} + \alpha d. \tag{5}$$

2.3 CALCULATION OF THE PHYSICAL QUANTITY

For calculation of permeability by MD simulation, the flow rate Q is obtained from the number of water molecules dN that pass through the slit in unit time dt.

$$Q = \frac{M}{\rho L_x N_A}\frac{dN}{dt}, \tag{6}$$

where M is the molecular weight of water; ρ, the molecular density of water; and N_A, Avogadro's constant. To ensure that the length in the depth direction (x axis direction in Figure. 1) does not become infinite, using the periodic boundary condition, Q is converted to be the flow rate per unit length in the x direction because equation (3) is based on the 2D model. The pressure is determined using the virial theorem:

$$\langle P \rangle = \frac{N k_B \langle T \rangle}{V}\frac{1}{3V}\sum_{i=1}^{N}\sum_{\substack{j=1 \\ j\neq i}}^{N'}\left\langle \mathbf{r}_{ij} \cdot \mathbf{F}_{ij} \right\rangle, \tag{7}$$

$$\mathbf{r}_{ij} = \mathbf{r}_i - \mathbf{r}_j \,, \tag{8}$$

where V is the volume of the system; T, the temperature of the system; k_B, the Boltzmann constant; N, the number of atoms; N', the number of atoms included in the periodic cells affecting the atom i; and $\mathbf{F}_{ij}$, the force induced by atom j on particle i. By applying equation(7) to the local region before and after passing through the graphene membranes, P_{before} and P_{after}, respectively, are obtained, and the difference between them is defined as ΔP.

$$\Delta P = P_{before} - P_{after} \tag{9}$$

3 MD MODEL

Our MD simulations are performed with the LAMMPS (Large-Scale Atomic-Molecular Massively Parallel Simulator) package[8]. The parameters are taken from the AMBER94 force field[9] and the detailed parameters are listed in Table 2. Note that the Lennard–Jones potential parameters for heterogeneous atoms are calculated using the Lorentz–Berthelot combining rules. Relaxation and flow simulations were performed in the NVT ensemble, and the temperature was maintained at 300 K using a Nosé–Hoover chain thermostat. Long-range Van der Waals forces were calculated by the cut-off method. Long-range Coulombic forces were calculated by the particle-particle particle-mesh method[10]. The SHAKE algorithm[11] was used to constrain the bonds and angles of oxygen and hydrogen in the water molecules and to prevent the time step from being too short. Other calculation conditions are listed in Table 2.

We focus on the system shown in Figure. 1. Two graphene membranes are located at the center of the unit cell (z = 5.0 nm) in parallel with width d. Seven values of d (= 0.464, 0.703, 0.8, 1.077, 1.677, 2.012, and 3,16 nm) were considered. The system dimensions were fixed at L_x = 1.845 nm and L_z = 10.00 nm, while L_y varied to 3d according to the slit width. When 3d was less than twice the cut-off distance, L_y was defined as $L_y \geq 2.737$ nm. Water molecules were located in the unit cell with a mass density of ρ = 1.0 g/cm^3 to simulate the properties of bulk water and the number of water molecules is varied from 1568 to 5156.

To calculate permeability, the flux through the slit and pressure difference should be known. We placed graphene walls at initial atomic coordinates of z = 0 and 10.0 nm and moved them at a constant velocity of v_p in the z direction as a piston to create a pressure difference. The physical quantities were calculated from stable values after 10 ps or more from the beginning of flow calculation. Ten values of v_p (= 0.00001 0.00002, 0.00003, 0.00004, 0.00005, 0.00006, 0.00007, 0.00008, 0.00009, and 0.0001 nm/fs) are were used to determine the pressure gradients. Periodic boundary conditions were applied in the x and y directions, and non-periodic boundary conditions were applied in the z direction so that the water near the graphene walls did not interact through the periodic cells. Each of the carbon atoms constituting the graphene slits was fixed at a hypothetical point, namely, $C_{virtual}$, to prevent the carbon atoms from being carried by the water flow. Because $C_{virtual}$ only affected the corresponding carbon atom and did not change the coordinates and velocity, the graphene membranes could be fixed without affecting other atoms.

Atomic Parameters				
Atom	ε[kcal/mol]	σ[Å]	mass[g/mol]	q[e]
C	0.0859	3.3997	12.0107	0.0
H	0.0000	0.0000	1.008	+0.52
O	0.1520	3.5366	15.9994	-1.04
Bond Parameters				
Bond	K_r[kcal/(mol·Å^2)]		r_{eq}[Å]	
C-C	469.0		1.42	
C-$C_{virtual}$	100.0		0.0	
O-H	553.0		0.9572	
Angle Parameter				
Angle	K_θ[kcal/(mol·radian^2)]		θ_{eq}[°]	
H-O-H	100.0		104.52	

Table 2: Potential energy function parameters for AMBER94.

NVT external thermostat temperature [K]	300
NVT damping constant [fs]	100.0
Timestep [fs]	1.0
Relaxation time [ps]	1000
Flow simulation time [ps]	50~500
van der Waals cutoff [Å]	8.0
Coulombic cutoff [Å]	8.0
Accuracy tolerance of SHAKE solution [Å^2]	0.0001

Table 3: Parameters of calculation.

4 RESULTS AND DISCUSSIONS

Snapshots of flow simulations for slits widths d = 0.464 and 3.16 nm (Kn = 0.65 and 0.095) and a piston velocity of v_p = 0.0001 nm/fs are shown in Figure 2. When d is small, i.e., Kn = 0.65, only one water molecule can pass through the membrane at a time, and a low-density region is observed after each water molecule passes through the membrane. This is a characteristic behavior of non-continuum flow and this behavior is not observed for Kn = 0.095, i.e., when d is large. Therefore, flow tendency changes within the measurement range (0.095 < Kn < 0.65). Given that this range is the transition regime, the flow form changes from a slip flow to a free-molecular flow as d decreases.

We calculated the relationships between d and α. The tendency of α changes at d = 0.8 nm (Kn = 0.375). Before and after at d = 0.8 nm, α does not change because of changes in d. We attribute this result to the transition to free-molecular flow. We defined the mean value of α at d < 0.8 nm as α_1 and that at d > 0.8 nm as α_2. Note that α_2 is approximately twice α_1, and the change in α at d = 0.8 nm is not caused by error. Therefore, the flow in the range Kn < 0.375 is a slip flow and that in the range Kn > 0.375 is a free-molecular flow.

Further, we calculated the relative error of permeability between the theoretical models and the MD measurements for each d. For theoretical model calculations, considering the region where water molecules can not exist owing to the repulsive forces between C and O atoms, we used the value obtained by subtracting the van der Waals diameter of a carbon atom (= 0.33997 nm) from the distance between the carbon atoms at the end of the slits. The relative errors of the non-slip model are greater than 0.45

for all d, and as d increases, the relative errors tend to decrease. This observation is supported by the right side of equations (3) and (5): the influence of the walls become relatively small as d increases. For $d > 0.8$ nm, the mean value of relative error of the slip-condition model ($\alpha = \alpha_2$) is 0.15, i.e., this error is small, and the MD simulation results show good agreement with the theoretical model of the slip condition ($\alpha = \alpha_2$). Therefore, it is reasonable that the slip model is expressed by equation (5). However, for $d < 0.8$ nm, the mean value of the relative error of the non-slip model is 0.92, and that of the slip-condition model ($\alpha = \alpha_1$) is 1.12. Compared with the models for $d > 0.8$ nm, those for $d < 0.8$ nm have a significantly large error. Consequently, the slip-condition model ($\alpha = \alpha_1$) and the non-slip model are not applicable in the range $d < 0.8$ nm ($Kn > 0.375$), and we suggest that the continuum-dynamics laws are also inapplicable in this range.

Finally, we calculated the density profile of water molecules passing through slits with $d = 0.703$, 0.8, and 1.077 nm to investigate the phenomena occurring near $d = 0.8$ ($Kn = 0.375$). For $d = 0.703$ nm, a high-density peak ($\rho > 1.5$ g/cm^3) was observed at approximately 0.35 nm from the edge, and for $d =$ 1.077 nm, two peaks were observed at approximately 0.35 and 0.73 nm from the edge. Therefore, considering the exclusive region corresponding to the van der Waals diameter of carbon atoms, high-density layers formed at approximately 0.3 nm from the both ends of the slit. On the other hand, for $d =$ 0.8 nm, such a high-density peak was not observed. Consequently, the high-density layers observed at both ends of the slit are considered to start overlapping when $d < 0.8$ nm, and for $d < 0.703$ nm, this layers overlap completely, forming one layer. The above discussions show that the flow form changes from a slip flow to a free-molecular flow when the high-density layers overlap, i.e., at $Kn = 0.375$, and this value of Kn is considered to be related to the application limit of the continuum dynamics law.

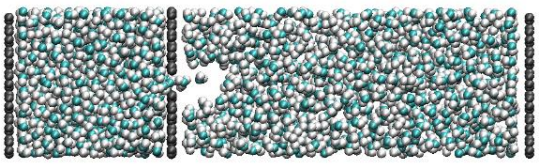

(a) $d = 0.464$ nm

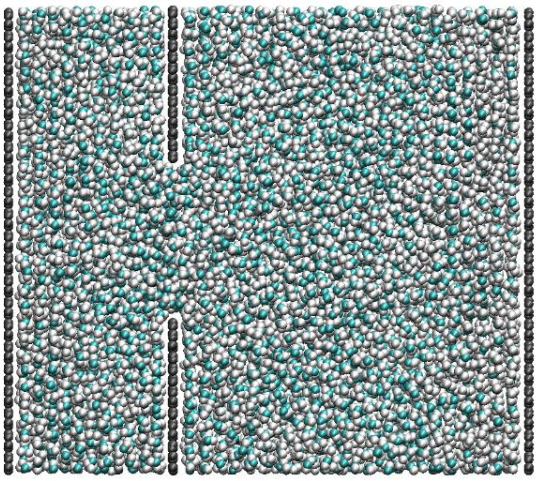

(b) $d = 3.16$ nm

Figure 2: Snapshots of flows through the slit in the graphene membrane.

5 CONCLUSIONS

In this study, we simulated water permeation through a graphene slit. The permeability predictions based on MD showed good agreement with the results of the slip-condition model for $Kn < 0.375$; however, for $Kn > 0.375$, the two sets of results differ. Additionally, water molecules form high-density layers at certain distances from the end of the slit, and the flow form changes from a slip flow to a free-molecular flow when the number of high-density layers decreases from two to one.

REFERENCES

[1] X. Wang, L. Zhi and K. Müllen, Transparent, conductive graphene electrodes for dye-sensitized solar cells, *Nano Letters,* **8**, 2008, pp. 323-327.

[2] Y. Liu, D. Yu, C. Zeng, Z. Miao and L. Dai, Biocompatible graphene oxide-based glucose biosensors, *Langmuir*, **26**, 2010, pp. 6158-6160.

[3] T. Ramanathan, A. A. Abdala, S. Stankovich, D. A. Dikin, M. Herrera-Alonso, R. D. Piner, *et al.*, Functionalized graphene sheets for polymer nanocomposites, *Nature Nanotechnology,* **3**, 2008, pp. 327-331.

[4] R. R. Nair, H. A. Wu, P. N. Jayaram, I. V. Grigorieva and A. K. Geim, Unimpeded Permeation of Water Through Helium-Leak-Tight Graphene-Based Membranes, *Science,* **335**, 2012, pp. 442-444.

[5] T. Tajiri, R. Matsuzaki and Y. Shimamura, Simulation of water impregnation through vertically aligned CNT forests using a molecular dynamics method, *Scientific reports,* **6**, 2016, pp. 1-7.

[6] M. Gad-el-hak, The fluid mechanics of microdevices — The Freeman Scholar Lecture, *Journal of Fluids Engineering,* **121**, 1999, pp. 5-33.

[7] H. Hasimoto, On the flow of a viscous fluid past a thin screen at small Reynolds numbers, *Journal of the Physical Society of Japan,* **13**, 1958, pp. 633-639.

[8] S. Plimpton, Fast Parallel Algorithms for Short-Range Molecular Dynamics, *Journal of Computational Physics,* **117**, 1995, pp. 1-19.

[9] W. D. Cornell, P. Cieplak, C. I. Bayly, I. R. Gould, K. M. Merz, D. M. Ferguson, *et al.*, A second generation force field for the simulation of proteins, nucleic acids, and organic molecules, *Journal of the American Chemical Society,* **117**, 1995, pp. 5179-5197.

[10] T. Darden, D. York and L. Pedersen, Particle mesh Ewald: An N·log(N) method for Ewald sums in large systems, *The Journal of Chemical Physics,* **98**, 1993, pp. 10089-10092.

[11] J.-P. Ryckaert, G. Ciccotti and H. J. Berendsen, Numerical integration of the cartesian equations of motion of a system with constraints: molecular dynamics of n-alkanes, *Journal of Computational Physics,* **23**, 1977, pp. 327-341.